Supporting information

Phosphate modification of Pd/Al_2O_3 enhances activity and stability in aromatic hydrogenation under CO-contaminated hydrogen

Adrian Seitz[1], Yaoci Sheng[2], Ian Backes[1], Phillip Nathrath[1], Dennis Weber[1,3], Tanja Franken[1,3], Roberto Félix[4], Angelo Rillera[4], Johannes Frisch[4,5], Marcus Bär[4,5,6,7], Tanja Retzer[2], Patrick Schühle[1,*]

[1]Institute of Chemical Reaction Engineering, Friedrich-Alexander-Universität Erlangen-Nürnberg, Egerlandstraße 3, 91058 Erlangen, Germany

[2]Interface Research and Catalysis, ECRC, Friedrich-Alexander-Universität Erlangen-Nürnberg, Egerlandstraße 3, 91058 Erlangen, Germany

[3]Technical Chemistry I, Technische Universität Darmstadt, Peter-Grünberg-Straße 8, 64287 Darmstadt, Germany

[4]Department Interface Design, Helmholtz-Zentrum Berlin für Materialien und Energie GmbH (HZB), Albert-Einstein-Straße 15, 12489 Berlin, Germany

[5]Energy Materials In-Situ Laboratory Berlin (EMIL), Helmholtz-Zentrum Berlin für Materialien und Energie GmbH (HZB), Albert-Einstein-Straße 15, 12489 Berlin, Germany

[6]Lehrstuhl für Physikalische Chemie II, Friedrich-Alexander-Universität Erlangen-Nürnberg, Egerlandstraße 3, 91058 Erlangen, Germany

[7]Department for X-ray Spectroscopy at Interfaces of Thin Films, Helmholtz-Institute Erlangen-Nürnberg for Renewable Energy, Albert-Einstein-Str. 15, 12489 Berlin, Germany

[*]patrick.schuehle@fau.de

Gas compositions during hydrogenation with impure H_2

Table S1: Partial pressures and concentrations in hydrogenation experiments with impure H_2. $p_{tot,mixed}$: total pressure of mixture added to reactor; $c_{i,mixed}$: concentration of compound i in mixture; $p_{i,mixed}$: calculated partial pressure of compound i added via mixture; $p_{H2,pure}$: H_2 pressure added to reactor via pure H_2; $p_{H2,tot}$: total H_2 pressure in reactor via mixture and pure H_2; $c_{i,reaction}$: calculated concentration of compound i during reaction; $c_{total\ impurities}$: total impurity concentration.

	H_2/CO	H_2/mixed – 12 %	H_2/mixed – 22 %	H_2/mixed – 36 %
$p_{tot,mixed}$ / bar	25.0	11.7	23.4	46.8
$c_{CO2,mixed}$ / vol%	-	32.0	32.0	32.0
$c_{CH4,mixed}$ / vol%	-	3.0	3.0	3.0
$c_{CO,mixed}$ / vol%	2.0	1.0	1.0	1.0
$c_{H2,mixed}$ / vol%	98.0	64.0	64.0	64.0
$p_{CO2.mixed}$ / bar	-	3.7	7.5	15.0
$p_{CH4.mixed}$ / bar	-	0.4	0.7	1.4
$p_{CO.mixed}$ / bar	0.5	0.1	0.2	0.5
$p_{H2,mixed}$ / bar	24.5	7.5	15.0	30.0
$p_{H2,pure}$ / bar	5.5	22.5	15.0	-
$p_{H2,tot}$ / bar	30.0	30.0	30.0	30.0
$c_{CO2,reaction}$ / vol%	-	10.9	19.5	32.0
$c_{CH4,reaction}$ / vol%	-	1.0	1.8	3.0
$c_{CO,reaction}$ / vol%	1.6	0.3	0.6	1.0
$c_{total\ impurities}$ / vol%	1.6	12.3	21.9	36.0
$c_{H2,reaction}$ / vol%	98.4	87.7	78.1	64.0

Synthesis and XRD of Pd_3P/SiO_2

A commercial SiO_2 powder (Thermo Scientific) was impregnated with a specific amount of $Pd(NO_3)_2 \cdot 2H_2O$ (Merck KGaA) in aqueous solution to reach 4 wt% Pd loading. After drying, the powder was calcined in 70 mL min^{-1} air for 2 hours at 400 °C (10 K min^{-1}). The calcined Pd/SiO_2 was impregnated with H_3PO_3 in aqueous solution to reach $n_P:n_{Pd} = 4$. After drying, the powder was reduced in a tubular furnace in a 10% H_2/N_2 mixture (total flow: 500 mL min^{-1}) for 2 hours at 400 °C (10 K min^{-1}).

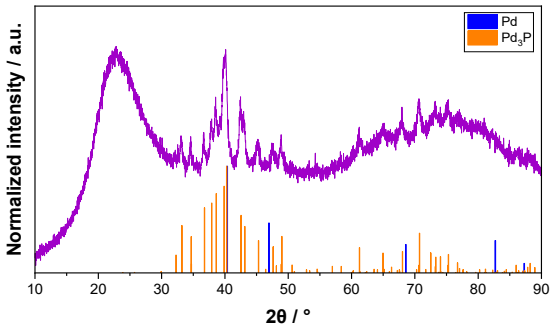

Figure S1: XRD patterns of Pd_3P/SiO_2 with Pd and Pd_3P reference.

In situ DRIFTS procedure

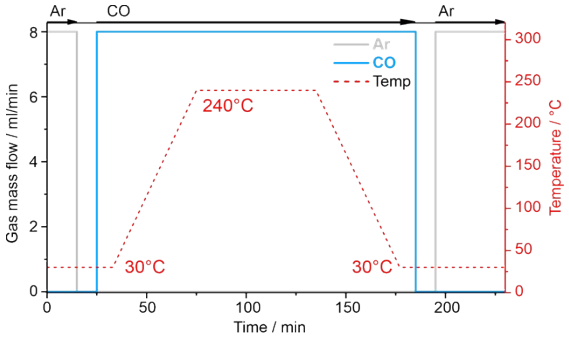

Figure S2: Schematic representation of the experimental procedure applied in the *in situ* DRIFTS experiments.

Synthesis and performance of H_3PO_3-modified Pd/SiO_2 and Pd/C

A commercial SiO_2 powder (Thermo Scientific) was impregnated with a specific amount of $Pd(NO_3)_2 \cdot 2H_2O$ (Merck KGaA) in aqueous solution to reach 4 wt% Pd loading. After drying, the powder was calcined in 70 mL min^{-1} air for 2 hours at 400 °C (10 K min^{-1}). To yield Pd/SiO_2, the powder was reduced in a tubular furnace in a 10% H_2/N_2 mixture (total flow: 500 mL min^{-1}) for 2 hours at 400 °C (10 K min^{-1}). For H_3PO_3 modification, the calcined Pd/SiO_2 powder was impregnated with H_3PO_3 in aqueous solution to reach the desired $n_P:n_{Pd}$. After drying, the powder was reduced in a tubular furnace in a 10% H_2/N_2 mixture (total flow: 500 mL min^{-1}) for 2 hours at 600 °C (10 K min^{-1}).

A commercial Pd/C powder catalyst containing 4 wt% Pd was purchased (Merck KGaA) and used as received. For H_3PO_3 modification, Pd/C powder was impregnated with H_3PO_3 in aqueous solution to reach the desired $n_P:n_{Pd}$. After drying, the powder was reduced in a tubular furnace in a 10% H_2/N_2 mixture (total flow: 500 mL min^{-1}) for 2 hours at 600 °C (10 K min^{-1}).

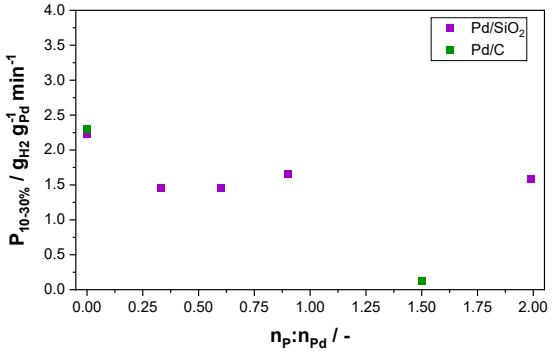

Figure S3: $P_{10–30\%}$ of Pd/SiO_2 and Pd/C (unmodified and modified with H_3PO_3) during H0-BT hydrogenation at 240 °C, 30 bar H_2-pressure and $n_{Pd}:n_{H0\text{-}BT} = 4.1 \cdot 10^{-4}$ at different $n_P:n_{Pd}$ ratios.

Variation of n_P:n_{Pd} with lot 2 of commercial Pd/Al_2O_3

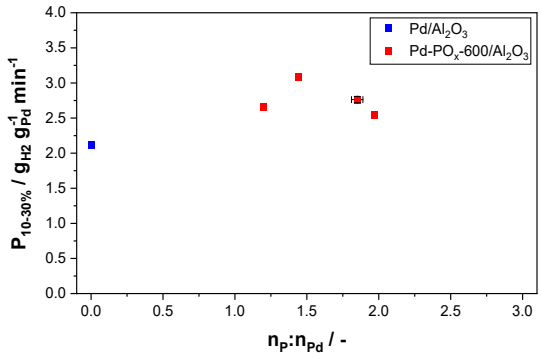

Figure S4: $P_{10–30\%}$ of Pd/Al_2O_3 and $Pd\text{-}PO_x\text{-}600/Al_2O_3$ during H0-BT hydrogenation at 240 °C, 30 bar H_2-pressure and n_{Pd}:$n_{H0\text{-}BT}$ $= 4.1 \cdot 10^{-4}$ at different n_P:n_{Pd} ratios (lot 2).

Kinetics under pure H_2

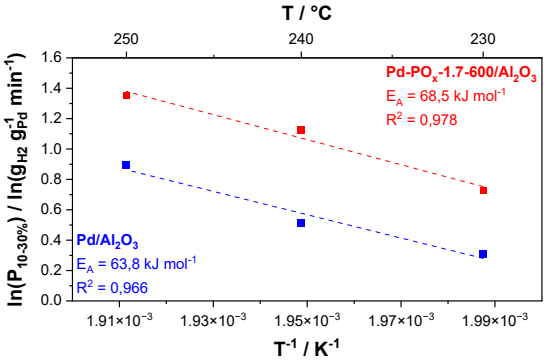

Figure S5: Arrhenius plot for Pd/Al_2O_3 (lot 1) and $Pd\text{-}PO_x\text{-}1.7\text{-}600/Al_2O_3$ (n_P:n_{Pd} = 1.7±0.3, lot 2) during H0-BT hydrogenation at 230-250 °C, 30 bar H_2-pressure and n_{Pd}:$n_{H0\text{-}BT}$ = $4.1 \cdot 10^{-4}$.

Productivity comparison with literature under CO-contaminated H_2

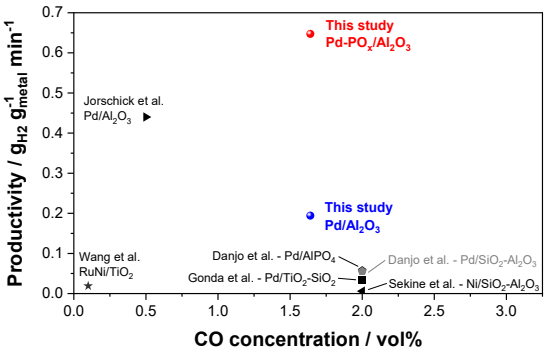

Figure S6: Productivity for hydrogenation of aromatic rings in $g_{H2}g_{metal}^{-1}min^{-1}$ over CO concentration for different catalysts from literature and this study.[1–5] More information regarding reaction conditions are given in Table S2.

Table S2: Catalyst, reaction temperature and substrate for hydrogenation of the respective studies from Figure S6.

Study	Catalyst	Temperature / °C	Substrate	Comment
Wang et al.[2]	RuNi/TiO_2	170	Toluene	Decreasing activity at > 170 °C
Jorschick et al.[3]	Pd/Al_2O_3	240	Dibenzyltoluene	
Danjo et al.[4]	Pd/$AlPO_4$	150	Naphthalene	
Danjo et al.[4]	Pd/SiO_2-Al_2O_3	150	Naphthalene	
Gonda et al.[5]	Pd/TiO_2-SiO_2	200	Toluene	
Sekine et al.[1]	Ni/SiO_2-Al_2O_3	155	Naphthalene	
This study	Pd/Al_2O_3	240	Benzyltoluene	
This study	Pd-PO_x/Al_2O_3	240	Benzyltoluene	

Effect of CO_2 and CH_4

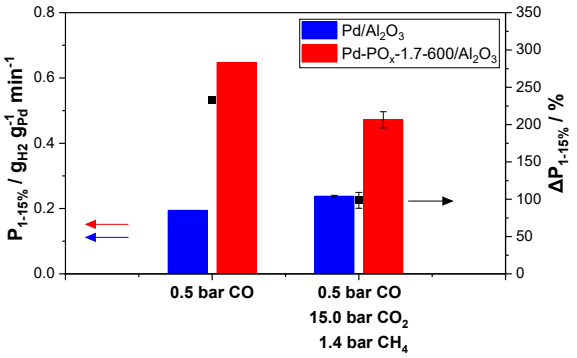

Figure S7: $P_{1–15\%}$ and $\Delta P_{1–15\%}$ of Pd/Al_2O_3 and $Pd\text{-}PO_x\text{-}1.7\text{-}600/Al_2O_3$ ($n_P:n_{Pd}$ = 1.7±0.3) during H0-BT hydrogenation with H_2/CO and H_2/mixed at 240 °C, 30 bar H_2-pressure, different impurity partial pressures, $n_{Pd}:n_{H0\text{-}BT} = 5.1 \cdot 10^{-4}$ for H_2/CO or $4.1 \cdot 10^{-4}$ for H_2/mixed (lot 2).

N_2 physisorption

Table S3: BET surface area, total pore volume and average pore diameter of Pd/Al_2O_3 and $Pd\text{-}PO_x\text{-}1.7\text{-}600/Al_2O_3$ (lot 2).

	BET surface area / $m^2\ g^{-1}$	Total pore volume / $cm^3\ g^{-1}$	Average pore diameter / nm
Pd/Al_2O_3	114	0.273	9.59
$Pd\text{-}PO_x\text{-}1.7\text{-}600/Al_2O_3$	96.8	0.243	10.0

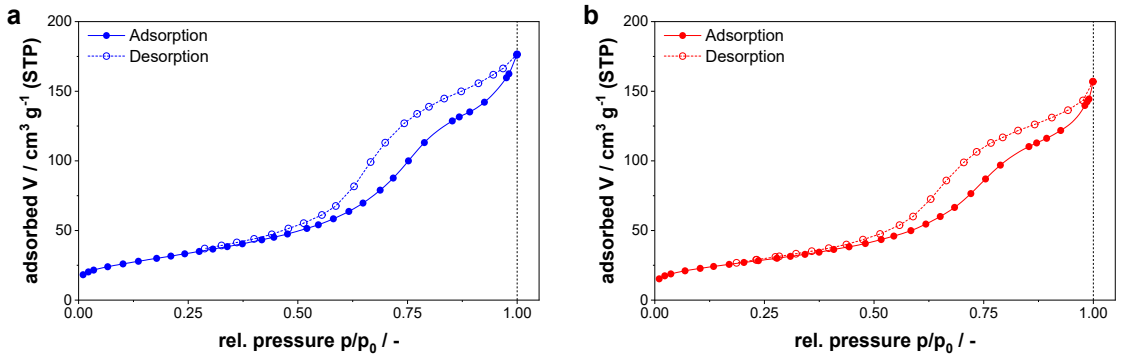

Figure S8: N_2 physisorption isotherms of (a) Pd/Al_2O_3 (b) $Pd\text{-}PO_x\text{-}1.7\text{-}600/Al_2O_3$ corresponding to the results shown in Table S3.

CO-pulse chemisorption

Table S4: Pd dispersion according to CO-pulse chemisorption for Pd/Al_2O_3, $Pd\text{-}600/Al_2O_3$ and $Pd\text{-}PO_x\text{-}1.7\text{-}600/Al_2O_3$ (lot 2).

	Pd dispersion according to CO-pulse chemisorption / %
Pd/Al_2O_3	18.5
$Pd\text{-}600/Al_2O_3$	12.2
$Pd\text{-}PO_x\text{-}1.7\text{-}600/Al_2O_3$	13.0

HR-TEM

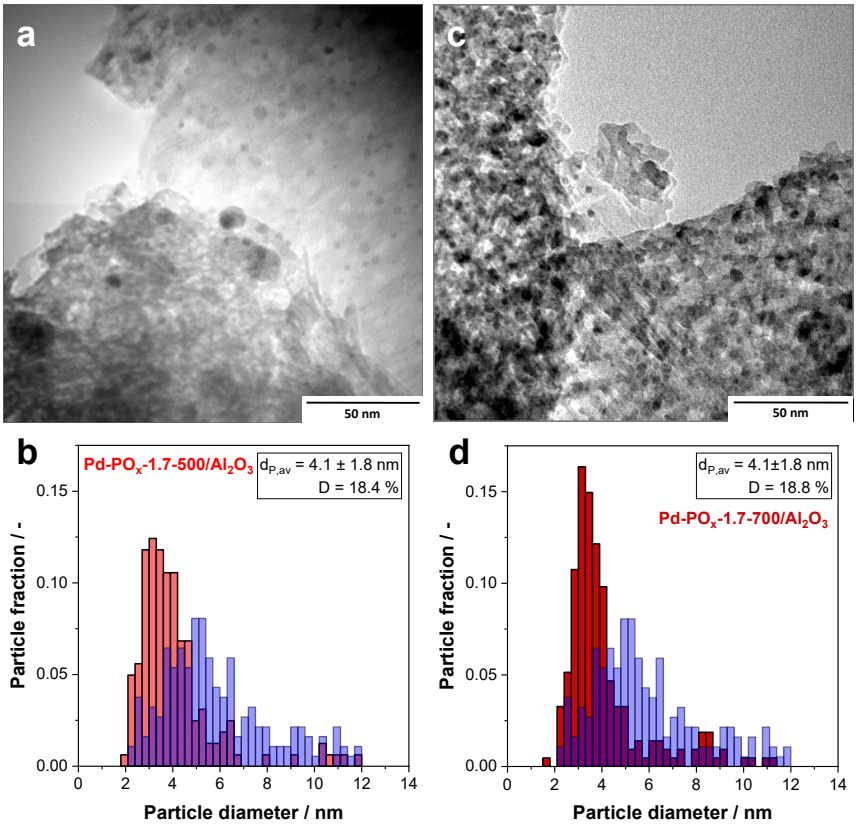

Figure S9: HR-TEM and particle size distribution of (a,b) Pd-PO$_x$-1.7-500/Al$_2$O$_3$ and (c,d) Pd-PO$_x$-1.7-700/Al$_2$O$_3$ (lot 2).

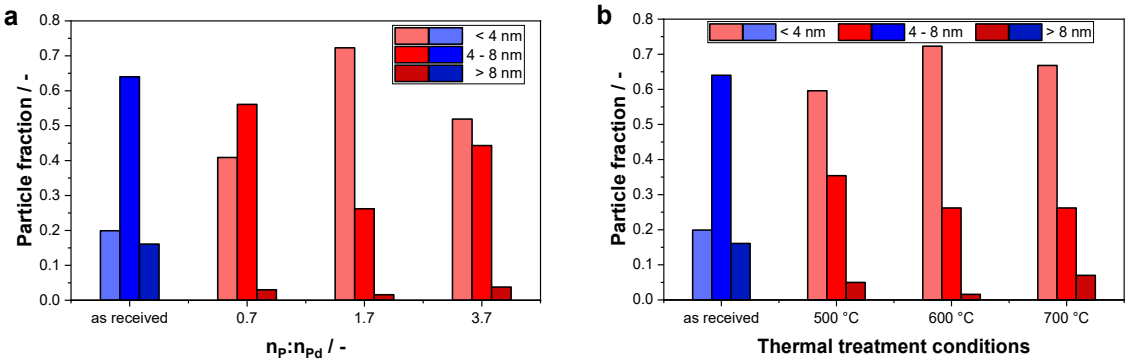

Figure S10: Fraction of particles <4 nm, 4-8 nm and >8 nm of (a) Pd/Al$_2$O$_3$ and Pd-PO$_x$-600/Al$_2$O$_3$ with different n$_P$:n$_{Pd}$ ratios (based on data from Figure 7) and (b) Pd/Al$_2$O$_3$ and Pd-PO$_x$-1.7/Al$_2$O$_3$ with varied thermal treatment temperature (n$_P$:n$_{Pd}$ = 1.7±0.3; based on data from Figure 7 and Figure S9).

XANES & EXAFS

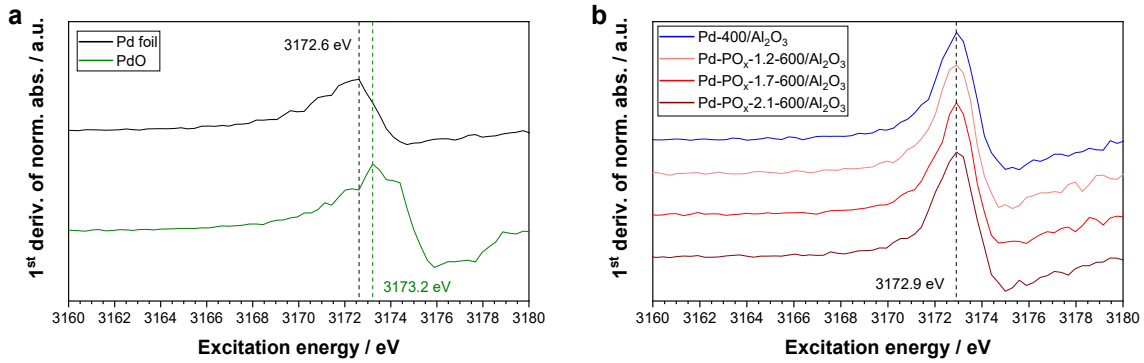

Figure S11: 1st derivative of normalized Pd L_3-edge XANES spectra of (a) Pd foil, PdO and (b) Pd-400/Al_2O_3, Pd-PO_x-1.2-600/Al_2O_3, Pd-PO_x-1.7-600/Al_2O_3 and Pd-PO_x-2.1-600/Al_2O_3 (from Figure 8a; lot 2). The dashed lines and given excitation energies correspond to the obtained edge positions.

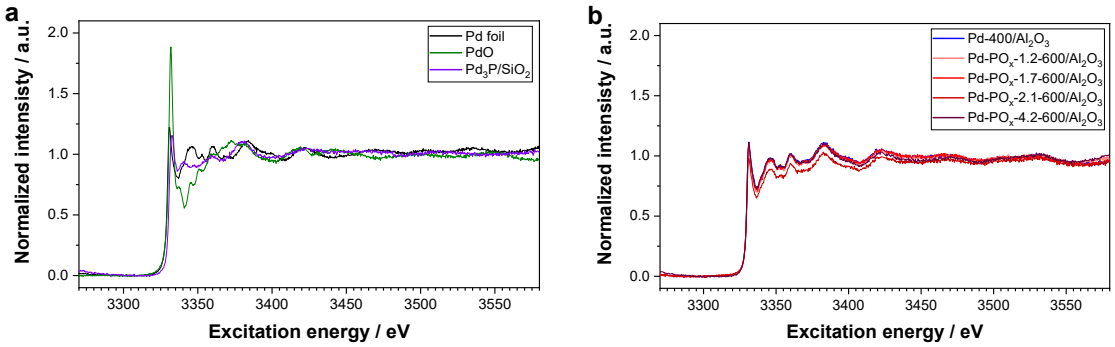

Figure S12: Normalized Pd L_2-edge EXAFS spectra of (a) Pd foil, PdO, Pd_3P/SiO_2, and (b) Pd-400/Al_2O_3, Pd-PO_x-1.2-600/Al_2O_3, Pd-PO_x-1.7-600/Al_2O_3, Pd-PO_x-2.1-600/Al_2O_3 and Pd-PO_x-4.2-600/Al_2O_3 (lot 2).

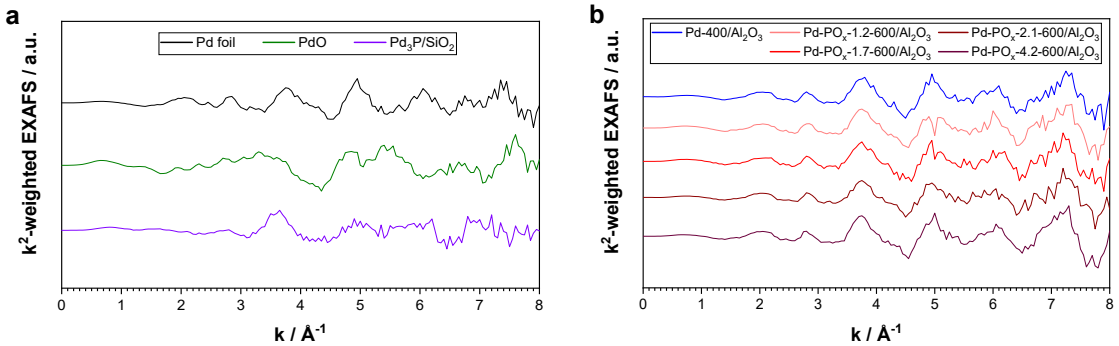

Figure S13: k^2-weighted Pd L_2-edge EXAFS spectra (k-space) of (a) Pd foil, PdO, Pd_3P/SiO_2, and (b) Pd-400/Al_2O_3, Pd-PO_x-1.2-600/Al_2O_3, Pd-PO_x-1.7-600/Al_2O_3, Pd-PO_x-2.1-600/Al_2O_3 and Pd-PO_x-4.2-600/Al_2O_3 (lot 2).

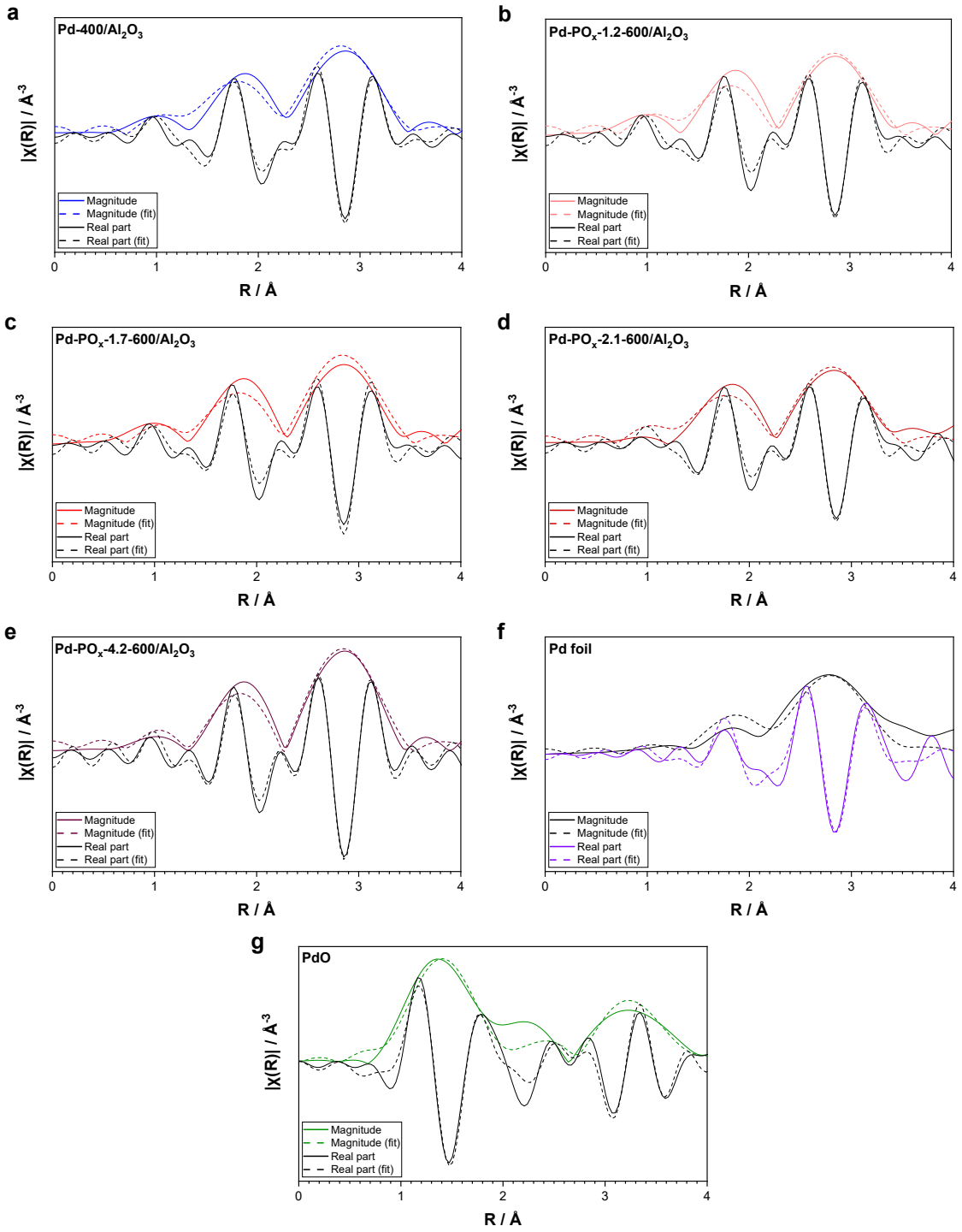

Figure S14: Fits of the EXAFS spectra of (a) Pd-400/Al_2O_3, (b) Pd-PO_x-1.2-600/Al_2O_3, (c) Pd-PO_x-1.7-600/Al_2O_3, (d) Pd-PO_x-2.1-600/Al_2O_3, (e) Pd-PO_x-4.2-600/Al_2O_3 (f) Pd foil and (g) PdO (lot 2).

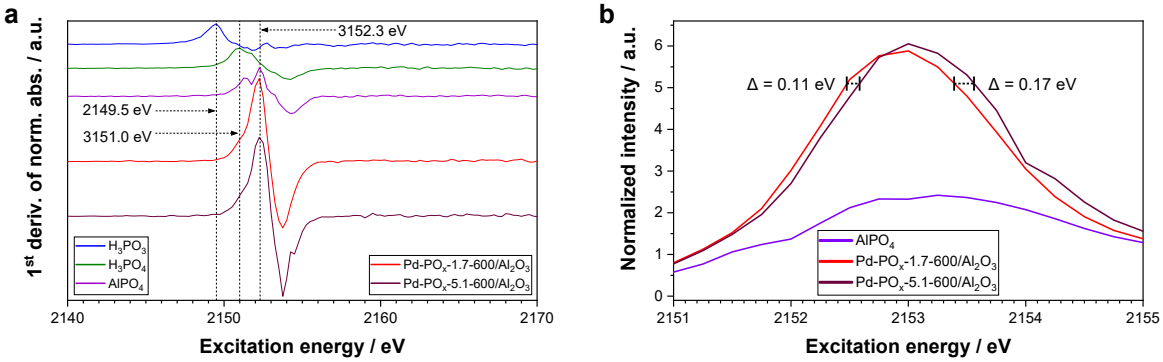

Figure S15: (a) 1st derivative of normalized P K-edge XANES spectra of H_3PO_3, H_3PO_4, $AlPO_4$, Pd-PO_x-1.7/Al_2O_3 and Pd-PO_x-5.1/Al_2O_3 (from Figure 9; lot 2). The dashed line and given excitation energies correspond to the obtained edge positions. (b) Zoom-in of normalized P K-edge XANES spectra of $AlPO_4$, Pd-PO_x-1.7-600/Al_2O_3 and Pd-PO_x-5.1-600/Al_2O_3 (from Figure 9; lot 2).

References

(1) Sekine, H.; Ohshima, M.; Kurokawa, H.; Miura, H. Liquid Phase Hydrogenation of Naphthalene in the Presence of CO over Supported Ni Catalyst. *React. Kinet. Catal. Lett.* **2008**, *95* (1), 99–105. https://doi.org/10.1007/s11144-008-5295-5.

(2) Wang, Z.; Dong, C.; Tang, X.; Qin, X.; Liu, X.; Peng, M.; Xu, Y.; Song, C.; Zhang, J.; Liang, X.; Dai, S.; Ma, D. CO-Tolerant RuNi/TiO2 Catalyst for the Storage and Purification of Crude Hydrogen. *Nat. Commun.* **2022**, *13* (1), 4404. https://doi.org/10.1038/s41467-022-32100-x.

(3) Jorschick, H.; Vogl, M.; Preuster, P.; Bösmann, A.; Wasserscheid, P. Hydrogenation of Liquid Organic Hydrogen Carrier Systems Using Multicomponent Gas Mixtures. *Int. J. Hydrog. Energy* **2019**, *44* (59), 31172–31182. https://doi.org/10.1016/j.ijhydene.2019.10.018.

(4) Danjo, Y.; Kikuchi, I.; Ino, Y.; Ohshima, M.; Kurokawa, H.; Miura, H. Support Effect of Pd/AlPO4 Catalyst in Hydrogen Storage of Organic Hydride Method in the Presence of CO. *React. Kinet. Mech. Catal.* **2012**, *105* (2), 381–389. https://doi.org/10.1007/s11144-011-0395-z.

(5) Gonda, M.; Ohshima, M.; Kurokawa, H.; Miura, H. Toluene Hydrogenation over Pd and Pt Catalysts as a Model Hydrogen Storage Process Using Low Grade Hydrogen Containing Catalyst Inhibitors. *Int. J. Hydrog. Energy* **2014**, *39* (29), 16339–16346. https://doi.org/10.1016/j.ijhydene.2014.07.158.